Catalysis Letters 59 (1999) 39–44

Acid- and base-treated Fe^{3+}–TiO_2-pillared clays for selective catalytic reduction of NO by NH_3

R.Q. Long and R.T. Yang *

Department of Chemical Engineering, University of Michigan, Ann Arbor, MI 48109-2136, USA
E-mail: yang@umich.edu

Received 7 December 1998; accepted 12 March 1999

Fe^{3+}-ion-exchanged delaminated pillared clays (PILCs) have been found previously to be more active than the vanadia-based catalysts for selective catalytic reduction (SCR) of NO by NH_3. The effects of acid treatment of the clay (before pillaring) and base treatments of the TiO_2-PILC (before ion exchange) on the activities of the Fe–TiO_2-PILC catalysts were studied. It was found that the acid treatment increased the activity (by 33%), but the base treatments decreased the activity (although they increased the cation exchange capacity of the pillared clay and, hence, the Fe content). The activities of the catalysts were directly related to their surface Brønsted acidities as identified by FT-IR of chemisorbed NH_3.

Keywords: selective catalytic reduction of NO, SCR of NO by NH_3, pillared clay for SCR, base-treated pillared clay, acid-treated pillared clay

1. Introduction

Selective catalytic reduction (SCR) of NO_x ($x = 1, 2$) with ammonia has been studied extensively because of its environmental importance. The commercial catalysts are V_2O_5 mixed with WO_3 and/or MoO_3 supported on TiO_2 [1,2]. The mechanism of the reaction on V_2O_5/TiO_2 is extensively studied and several different mechanisms have been proposed [1–10]. Although the vanadium-based catalysts are highly active, major disadvantages remain, such as their toxicity and high activities for oxidation of SO_2 to SO_3. Hence there are continuing efforts for developing new catalysts [1]. Pillared clays are particularly promising [11–17].

Pillared interlayer clays (PILCs), or pillared clays, are two-dimensional layered materials. Both Brønsted and Lewis acid sites exist in pillared clays. PILCs and metal-oxide-doped PILCs were studied as catalysts in the SCR reaction in our previous studies [11–15]. More recently, we have found that Fe-exchanged TiO_2-PILC catalysts have higher activities and N_2 product selectivities than the vanadia-based catalysts. Moreover, the catalytic activities were increased by the presence of H_2O and SO_2, which was attributed to the increase in Brønsted acidity of the catalysts [17]. Both Fe^{3+} ions and Brønsted acidity are important for the SCR reaction on the Fe–TiO_2-PILC catalysts.

It has been reported that base (e.g., NH_3 and NaOH) treatments could increase the cation exchange capacity (CEC) of pillared clays [18,19], and that acid treatment of the clay before pillaring could increase the Brønsted acidity of the PILCs [20,21]. In this study we investigated the effects of acid/base treatments of, respectively, clay/TiO_2-PILC, on the SCR activities of the Fe–TiO_2-PILC catalyst.

2. Experimental

Delaminated TiO_2-PILC was synthesized by following the procedure described in detail elsewhere [17]. The starting clay was a purified-grade bentonite powder from Fisher Co. Base-treated TiO_2-PILCs were prepared according to the method given by Li et al. [19]. 4 g TiO_2-PILC was stored in a desiccator containing 150 ml 29.8% NH_4OH solution in a beaker. After exposure to ammonia vapor for 24 h at room temperature, the sample was washed to pH = 7 with deionized water. NaOH-treated TiO_2-PILC was prepared by mixing 2 g TiO_2-PILC with 100 ml 0.02 M NaOH solution for 1 h at room temperature, followed by washing with deionized water and dilute HCl. The two base-treated samples were then washed with 100 ml 1 M NH_4Cl solution followed by deionized water until the wash water was free of Cl^- ions (by using the silver nitrate test). Finally, the solids were dried overnight at 120 °C. Acid treatment of clay was accomplished by mixing 10 g bentonite with 200 ml 1 wt% H_2SO_4 solution at 95 °C for 16 h [21]. After filtering, the solid was washed until the water was SO_4^{2-} free (by using the barium chloride test) and dried at 120 °C for 12 h. The acid-treated bentonite was then used to synthesize TiO_2-pillared acid-treated clay [17]. The Fe-exchanged catalysts were prepared by using a conventional ion exchange procedure. In each case, 2 g sample, i.e., TiO_2-PILC, base-treated TiO_2-PILCs and TiO_2-pillared acid-treated clay, was added to 200 ml of 0.05 M $Fe(NO_3)_3$ solution followed by constant stirring for 6 h at room temperature. The pH values of the solutions were 1.5. The

* To whom correspondence should be addressed.

mixtures were then filtered and washed 5 times with deionized water. Finally, the obtained solid samples were dried at 120 °C in air for 12 h, then calcined at 400 °C for 6 h. These catalysts are designated as Fe–TiO_2-PILC, Fe–TiO_2-PILC (NH_3), Fe–TiO_2-PILC (NaOH) and Fe–TiO_2-PILC (H_2SO_4). The total iron contents in these samples were measured by neutron activation analysis.

Powder X-ray diffraction (XRD) was conducted with a Rigaku Rotaflex D/Max-C system with Cu K_α (λ = 0.1543 nm) radiation. The samples were loaded on a sample holder with a depth of 1 mm. XRD patterns were recorded in the range of 2θ = 2–45°. A Micromeritics ASAP 2010 micropore size analyzer was used to measure the N_2 adsorption isotherms of the samples at liquid-N_2 temperature (−196 °C). The specific surface areas of the samples were determined from the linear portion of the BET plots (P/P_0 = 0.05–0.20). The pore size distribution was calculated from the desorption branch of the N_2 adsorption isotherm using the Barrett–Joyner–Halenda (BJH) formula, because the desorption branch can provide more information on the degree of blocking than the adsorption branch. Prior to the surface area and pore size distribution measurements, the samples were degassed *in vacuo* at 350 °C for 6 h.

The SCR activity measurements were carried out in a fixed-bed quartz reactor. 0.2 g catalyst was used in this work. The flue gas was simulated by blending different gaseous reactants. Two sets of flowmeters were used to control the flowrates of the individual reactants. He, NH_3/He, and NO/He gases were controlled by rotameters, whereas SO_2/He and O_2 were controlled by mass flowmeters (FM 4575 Linde Division). The typical reactant gas composition was as follows: 1000 ppm NO, 1000 ppm NH_3, 2% O_2, 1000 ppm SO_2 (when used), 8% water vapor (when used), and balance He. The total flowrate was 500 ml/min (ambient conditions) and the GHSV (gas hourly space velocity) was 113 000 1/h. The premixed gases (1.01% NO in He, 1.00% NH_3 in He, and 0.99% SO_2 in He) were supplied by Matheson. Water vapor was generated by passing He through a heated gas-wash bottle containing deionized water. The tubings of the reactor system were wrapped with heating tapes to prevent formation and deposition of ammonium sulfate/bisulfate and ammonium nitrate. The NO and NO_2 concentrations were continually monitored by a chemiluminescent NO/NO_x analyzer (Thermo Electro Corp., model 10). To avoid errors caused by the oxidation of ammonia in the converter of the NO/NO_x analyzer, an ammonia trap containing phosphoric acid solution was installed before the sample inlet to the chemiluminescent analyzer. The products were also analyzed by a gas chromatograph (Shimadzu, 14A) at 50 °C with a 5A molecular sieve column for N_2 and a Porapak Q column for N_2O. Hence the nitrogen balance and the product selectivities for N_2 and N_2O could be obtained.

The surface acidity of the catalysts was measured by infrared spectra of NH_3-adsorbed samples on a Nicolet Impact 400 FT-IR spectrometer with a TGS detector. Self-supporting wafers of 1.3 cm diameter were prepared by pressing 20 mg samples and were loaded into a high temperature IR cell with BaF_2 windows. The wafers were treated at 450 °C for 30 min in a flow of He (99.9998%, 100 ml/min) and then cooled to room temperature, and the background spectra were recorded in He before ammonia adsorption. Adsorption of NH_3 was performed at room temperature in a flow of 1.00% NH_3/He (100 ml/min) for 30 min followed by purging for 15 min with He. All of the spectra were recorded by accumulating 100 scans at a spectral resolution of 4 cm^{-1}. The NH_3 adsorption on samples pretreated with H_2O and SO_2 at 400 °C was also studied in this work.

3. Results and discussion

X-ray powder diffraction patterns of Fe–TiO_2-PILC, Fe–TiO_2-PILC (NH_3), Fe–TiO_2-PILC (NaOH) and Fe–TiO_2-PILC (H_2SO_4) are shown in figure 1. The XRD patterns of the Fe-exchanged samples were similar to that of delaminated TiO_2-PILC which exhibited no (001) reflection [17]. The delaminated pillared clays usually show larger pore diameters than laminated pillared clays. Delamination will increase the diffusion rates for the SCR reaction. The peak at 19.7° was the summation of hk indices of (02) and (11) and that at 35.0° was the summation of hk indices of (13) and (20) [22]. The peaks at 25.3 and 26.5° came from (101) diffractions of anatase TiO_2 and quartz impurities, respectively. No peaks for iron oxide were detected.

The BET surface areas, pore volumes and pore size distributions of Fe–TiO_2-PILC and acid/base-treated samples

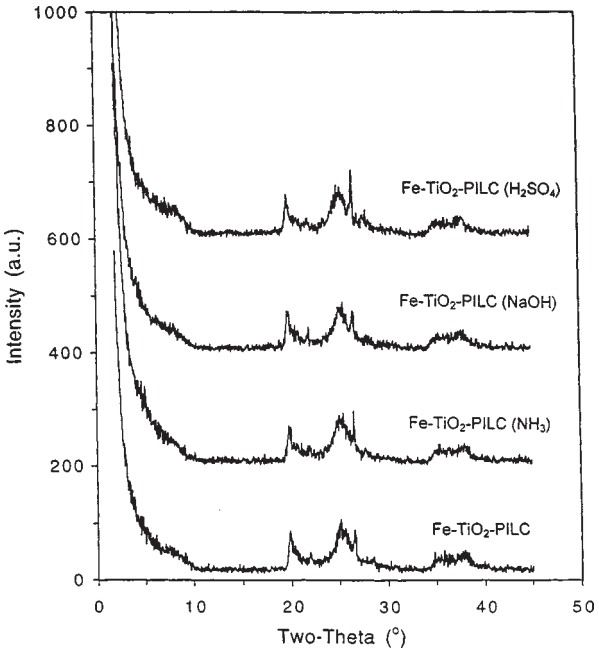

Figure 1. XRD patterns of the catalysts (see table 1 for sample designation).

Table 1
Characterization of the catalysts.

Sample	Fe content (wt%)	Surface area (m^2/g)	Pore volume (cm^3/g)	Bimodal pore diameters (nm)
Fe–TiO_2-PILC[a]	4.32	246	0.29	2.3, 3.7
Fe–TiO_2-PILC (NH_3)[b]	4.57	256	0.30	2.4, 3.8
Fe–TiO_2-PILC (NaOH)[c]	5.02	243	0.34	2.5, 3.8
Fe–TiO_2-PILC (H_2SO_4)[d]	4.25	225	0.30	2.4, 3.8

[a] TiO_2-PILC ion-exchanged with Fe^{3+}.
[b] TiO_2-PILC treated with NH_3, followed by Fe^{3+} ion exchange.
[c] TiO_2-PILC treated with NaOH, followed by Fe^{3+} ion exchange.
[d] Bentonite treated with H_2SO_4, then pillared with TiO_2, followed by Fe^{3+} ion exchange. See text for details.

are summarized in table 1. The surface areas and pore volumes of these samples were 225–256 m^2/g and 0.29–0.34 cm^3/g, respectively. Each of the samples showed a bimodal pore size distribution. The small pores appeared at ca. 2.4 nm and the big pores were ca. 3.8 nm. This indicates that the acid and base pretreatments did not significantly affect the pore structure of the Fe–TiO_2-PILC catalysts.

The iron content in TiO_2-PILC obtained by neutron activation analysis was 1.53 wt%. The ammonia and NaOH treatments did not change the value in the two base-treated samples. The iron content in TiO_2-pillared H_2SO_4-treated clay was 1.49 wt%. The total iron contents in the Fe-exchanged catalysts are shown in table 1. The Fe contents in the Fe^{3+}-exchanged catalysts were higher than that in the TiO_2-PILCs. As compared with Fe–TiO_2-PILC, the base treatment increased the CEC and iron contents in the Fe–TiO_2-PILC (NH_3) and Fe–TiO_2-PILC (NaOH) catalysts, and the increase in the CEC by the NaOH treatment was higher than that by the NH_3 treatment. The Fe content in Fe–TiO_2-PILC (H_2SO_4) was almost the same as that in Fe–TiO_2-PILC, suggesting that acid treatment of clay did not affect the CEC of TiO_2-PILC.

IR spectra of the ammonia adsorbed at room temperature on the Fe–TiO_2-PILC samples (that were pretreated at 450 °C in He for 30 min) are shown in figure 2. A strong band at 1452 cm^{-1} and three weaker bands at ca. 1682, 1596 and 1233 cm^{-1} were observed on the samples. The bands at 1682 and 1452 cm^{-1} were due to the symmetric and asymmetric bending vibrations of NH_4^+ that was chemisorbed on the Brønsted acid sites, while the bands at 1596 and 1233 cm^{-1} could be assigned to asymmetric and symmetric vibrations of the N–H bonds in NH_3 coordinately linked to Lewis acid sites [23,24]. For all the samples, there were more Brønsted acid sites than Lewis acid sites. When TiO_2-PILC was treated by NH_3 and NaOH, the intensities of the ammonia absorption bands on the Fe-exchanged samples were found to decrease as compared to Fe–TiO_2-PILC. In contrast, the Fe–TiO_2-PILC (H_2SO_4) had a slightly higher Brønsted acidity than Fe–TiO_2-PILC (figure 2). The NH_3 adsorption on the Fe–TiO_2-PILC catalysts pretreated with $SO_2 + O_2 + H_2O$ was also studied. The samples were treated at 400 °C for 15 min in flowing $SO_2 + O_2 + H_2O$/He (1000 ppm SO_2, 2% O_2 and 5% H_2O) followed by purging for 10 min by He, and then adsorbed NH_3 for 30 min at room temperature. Two strong bands at 1451 and 1238 cm^{-1} and two weak bands at 1682 and 1598 cm^{-1} were observed (figure 3). The band at around 1238 cm^{-1}, attributed to Lewis ammonia in figure 2, also existed on these samples before NH_3 adsorption (not shown). It is probably due to the combination band of sulfate species and Lewis ammonia [17,25]. As compared with figure 2, the NH_4^+ band at 1451 cm^{-1} was much stronger than that on the samples without sulfation, indicating that the treatment by $SO_2 + O_2 + H_2O$/He significantly increased the Brønsted acidity of the Fe–TiO_2-PILC samples. The Brønsted acidities of the sulfated samples followed the rank order (figure 3): Fe–TiO_2-PILC

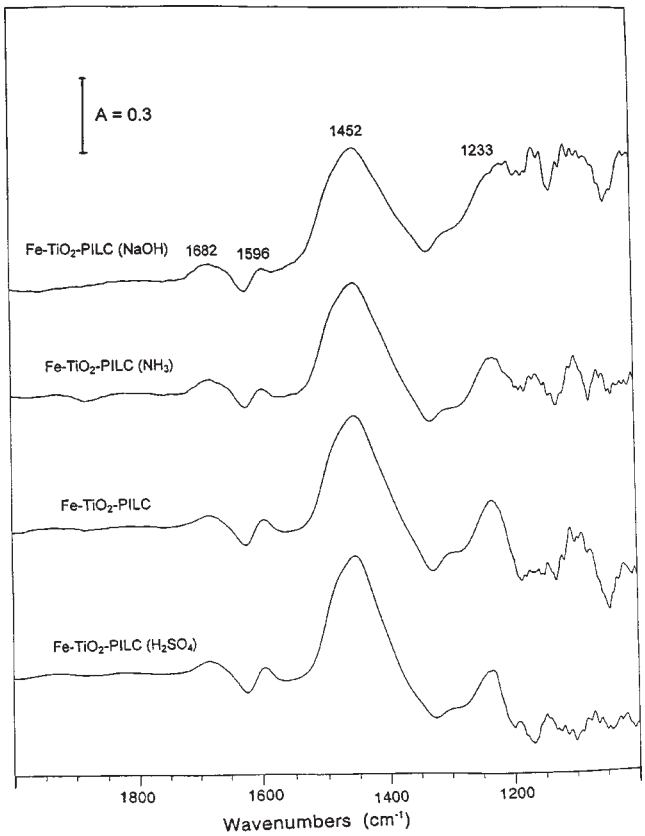

Figure 2. FT-IR spectra of chemisorbed NH_3 at 25 °C on the catalysts (see table 1 for sample designation).

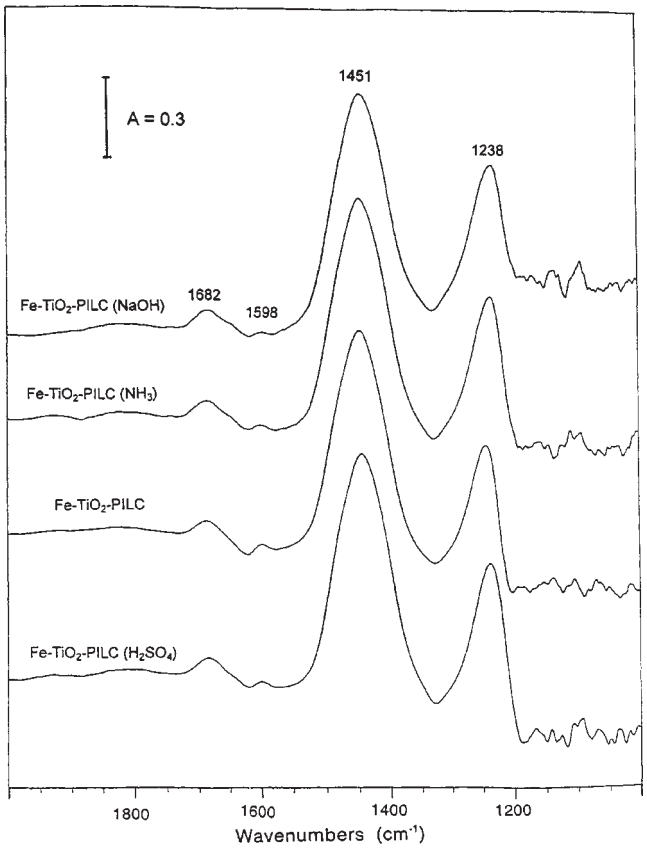

Figure 3. FT-IR spectra of chemisorbed NH_3 at 25 °C on the catalysts pretreated by $SO_2 + O_2 + H_2O$/He at 400 °C (see table 1 for sample designation).

(H_2SO_4) > Fe–TiO_2-PILC > Fe–TiO_2-PILC (NH_3) > Fe–TiO_2-PILC (NaOH).

The SCR activities of the Fe–TiO_2-PILC samples are summarized in tables 2 and 3. As indicated elsewhere [17], Fe–TiO_2-PILC was highly active in the SCR reaction and the activity increased with temperature from 300 to 450 °C (table 2). No detectable N_2O was formed by the catalyst. When TiO_2-PILC was pretreated by NH_3 and NaOH, the maximum activities of Fe–TiO_2-PILC (NH_3) and Fe–TiO_2-PILC (NaOH) decreased. In contrast, acid treatment of the clay increased the SCR activity since NO conversions on Fe–TiO_2-PILC (H_2SO_4) were higher than that on Fe–TiO_2-PILC. The effect of $H_2O + SO_2$ on SCR activity was also studied here. After 8% H_2O and 1000 ppm SO_2 were added to the reactants, NO conversions decreased at 300 °C on these catalysts (compare tables 2 and 3). This is mainly due to the inhibition by H_2O [17]. At temperatures above 350 °C, the catalytic activities increased significantly. The enhancement in activity by $H_2O + SO_2$ was attributed to the increase in Brønsted acidity resulting from the formation of sulfate species on the samples [17]. The maximum NO conversion also decreased in the order: Fe–TiO_2-PILC (NaOH) < Fe–TiO_2-PILC (NH_3) < Fe–TiO_2-PILC < Fe–TiO_2-PILC (H_2SO_4) in the presence of H_2O and SO_2. The nitrogen balance was above 96% in the work. The SCR activity can also be represented quantitatively by first-order rate constant (k) (since the reaction is known to be first order with respect to NO under stoichiometric NH_3 conditions on a variety of catalysts [1,2]). By assuming plug flow reactor (in a fixed bed of catalyst) and free of diffu-

Table 2
Catalytic performance of Fe–TiO_2-PILC catalysts (see table 1 for notation) in the absence of H_2O and SO_2.[a]

Catalyst	Temperature (°C)	NO conv. (%)	Selectivity (%)		k[b] (cm^3/g s)
			N_2	N_2O	
Fe–TiO_2-PILC	300	52.5	100	0	59.6
	350	78.5	100	0	134
	375	86.2	100	0	179
	400	90.0	100	0	217
	450	91.0	100	0	243
Fe–TiO_2-PILC (NH_3)	300	55.0	100	0	64.0
	350	78.0	100	0	132
	375	86.0	100	0	178
	400	88.0	100	0	199
	450	87.5	100	0	210
Fe–TiO_2-PILC (NaOH)	300	48.0	100	0	52.4
	350	70.8	100	0	107
	375	78.5	100	0	139
	400	81.5	99.8	0.2	159
	450	84.5	99.6	0.4	188
Fe–TiO_2-PILC (H_2SO_4)	300	55.0	100	0	64.0
	350	82.2	100	0	150
	375	90.0	100	0	209
	400	92.0	100	0	238
	450	90.5	99.8	0.2	238

[a] Reaction conditions: 0.2 g catalyst, [NO] = [NH_3] = 1000 ppm, [O_2] = 2%, He = balance, total flow rate = 500 ml/min and GHSV = 113 000 1/h.
[b] First-order rate constant, as defined in the text and calculated by equation (1).

Table 3
Catalytic performance of Fe–TiO_2-PILC catalysts (see table 1 for notation) in the presence of H_2O and SO_2.[a]

Catalyst	Temperature (°C)	NO_x conv. (%)	Selectivity (%)		k[b] (cm^3/g s)
			N_2	N_2O	
Fe–TiO_2-PILC	300	39.5	100	0	40.3
	350	90.0	100	0	201
	375	96.0	100	0	292
	400	98.1	100	0	373
	450	97.1	100	0	358
Fe–TiO_2-PILC (NH_3)	300	36.0	100	0	35.8
	350	88.5	100	0	188
	375	96.0	100	0	292
	400	97.0	100	0	330
	450	96.5	99.8	0.2	339
Fe–TiO_2-PILC (NaOH)	300	40.5	100	0	41.6
	350	80.5	100	0	142
	375	88.0	100	0	192
	400	92.0	99.8	0.2	238
	450	91.5	99.7	0.3	249
Fe–TiO_2-PILC (H_2SO_4)	300	41.5	100	0	42.9
	350	91.0	100	0	210
	375	98.0	100	0	354
	400	99.5	99.8	0.2	498
	450	99.0	99.7	0.3	465

[a] Reaction conditions: 0.2 g catalyst, $[NO] = [NH_3] = 1000$ ppm, $[O_2] = 2\%$, $[H_2O] = 8\%$, $[SO_2] = 1000$ ppm, He = balance, total flow rate = 500 ml/min and GHSV = 113 000 1/h.
[b] Same as defined in table 2.

sion limitation, the rate constant can be calculated from the NO_x conversion (X) by

$$k = -\frac{F_0}{[\mathrm{NO}]_0 W} \ln(1 - X), \qquad (1)$$

where F_0 is the molar NO feed rate, $[NO]_0$ is the molar NO concentration at the inlet (at the reaction temperature), and W is the catalyst amount (g). From the NO conversions and reaction conditions, first-order rate constants were calculated and compared in tables 2 and 3. Judging by the k values, as compared with the untreated Fe–TiO_2-PILC, the maximum SCR activity on Fe–TiO_2-PILC (H_2SO_4) increased 33%, but that on Fe–TiO_2-PILC (NH_3) and Fe–TiO_2-PILC (NaOH) decreased 9 and 33%, respectively. The maximum k value of Fe–TiO_2-PILC (H_2SO_4) was 2.6 times as active as the commercial-type $V_2O_5 + WO_3/TiO_2$ catalyst under the same conditions with SO_2 and H_2O (498 vs. 192 cm^3/g s at 400 °C [17]). It should be noted that, since pore diffusion resistance may be significant, k should be regarded as the overall rate constant which represents the overall activity (including pore diffusion resistance).

PILCs are prepared by exchanging the charge-compensating cations between the clay layers with larger inorganic hydroxyl metal cations (oligomers). Upon heating, the metal oligomers are decomposed to stable metal oxide pillars (and protons) which keep silicate layers separated and create interlayer spacing of molecular dimension. Meanwhile, some of the protons migrate from the interlayer surfaces to the octahedral layer within the clay layer where they neutralize the negative charges at the substitution cations (such as Mg^{2+} that substitutes Al^{3+}). Therefore, the CEC of PILCs decreases as compared with unpillared clays. However, base treatment can partially restore CEC of PILCs. The protons in the octahedral layer are retrieved to the surface by NH_3 to form NH_4^+ [18], while the treatment by NaOH can partially destroy the pillars and increase the CEC of PILCs [19]. As expected, the iron contents in Fe–TiO_2-PILC (NH_3) and Fe–TiO_2-PILC (NaOH) increased to 4.57 and 5.02%, respectively, from 4.32% in Fe–TiO_2-PILC (table 1). But the maximum SCR activities on the two base-treated samples were lower than that on Fe–TiO_2-PILC both in the presence and absence of H_2O and SO_2 (tables 2 and 3). The decrease in activity was consistent with the decrease in the Brønsted acidity of the samples (figures 2 and 3). The decrease in the Brønsted acidity might result from the fact that more H^+ ions were substituted by Fe^{3+} during the ion exchange step in the preparation of the catalysts. Moreover, NaOH treatment also neutralized some protons in TiO_2-PILC. On the other hand, the higher iron ion concentrations in the two base-treated catalysts would also increase non-selective reaction of NH_3 with O_2 at high temperatures and thus result in a decrease in NO conversions. By comparison, the acid-treated clay could increase the Brønsted acidity of PILC by removing some base oxides (e.g., Al_2O_3 and MgO) in the clay [20,21]. Consequently it enhanced the SCR activity of the Fe–TiO_2-PILC catalyst. The relationships between NO conversion and iron content and Brønsted acidity for the four Fe–TiO_2-PILC catalysts are shown in figure 4. It clearly shows that the NO conversion increased with an increase in Brønsted acidity, but decreased with increasing iron content on the four catalysts.

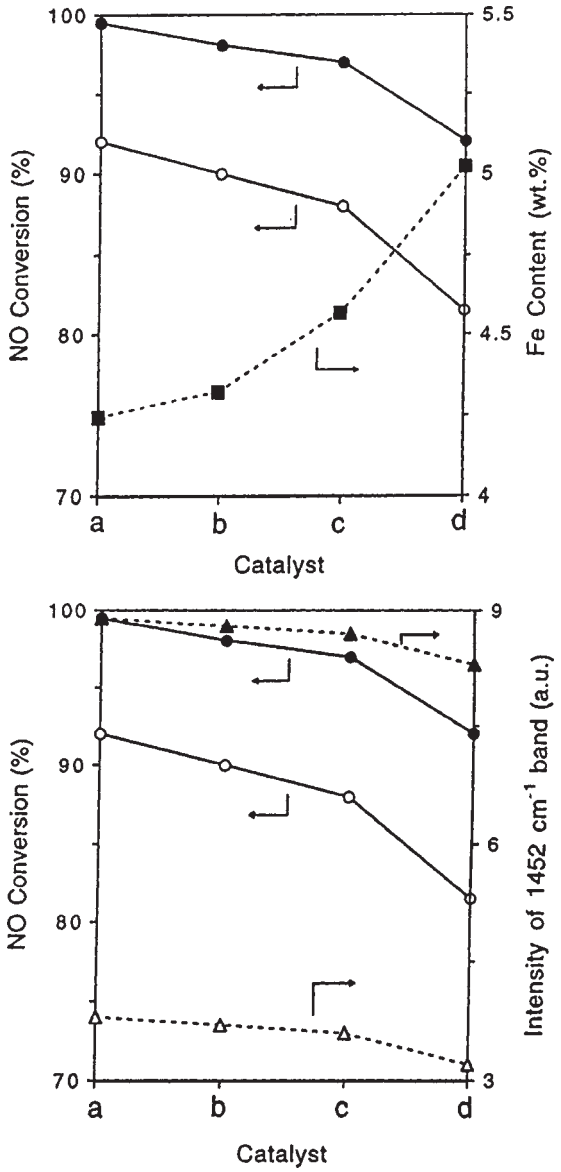

Figure 4. Relationship of NO conversion with iron content and Brønsted acidity (indicated by band intensity at 1452 cm^{-1}) of the catalysts (see table 1 for sample designation): (a) Fe–TiO_2-PILC (H_2SO_4), (b) Fe–TiO_2-PILC, (c) Fe–TiO_2-PILC (NH_3) and (d) Fe–TiO_2-PILC (NaOH). (●) NO conversion at 400 °C with $H_2O + SO_2$, (○) NO conversion at 400 °C without $H_2O + SO_2$, (■) Fe content, (△) Brønsted acidity and (▲) Brønsted acidity after sulfation.

4. Conclusions

Acid treatment of the clay before pillaring increased the SCR activity (by 33%) on Fe^{3+}-ion-exchanged TiO_2-PILC. Although base treatments of TiO_2-PILC increased its cation exchange capacity and, hence, the Fe^{3+} contents in the Fe–TiO_2-PILC catalysts, they decreased the catalytic activity for the SCR reaction. The SCR activity was directly related to the Brønsted acidity, not to the iron content of the Fe–TiO_2-PILC catalysts.

Acknowledgement

This work was supported by Electric Power Research Institute.

References

[1] H. Bosch and F. Janssen, Catal. Today 2 (1988) 369.
[2] G. Busca, L. Lietti, G. Ramis and F. Berti, Appl. Catal. B 18 (1998) 1.
[3] A. Miyamoto, K. Kobayashi, M. Inomata and Y. Murakami, J. Phys. Chem. 86 (1982) 2945.
[4] J.A. Odriozola, H. Heinemann, G.A. Somorjai, J.F. Garcia de la Banda and P. Pereira, J. Catal. 119 (1989) 71.
[5] M. Schramlmarth, A. Wokaun and A. Baiker, J. Catal. 124 (1990) 86.
[6] G. Ramis, G. Busca, F. Bregani and P. Forzatti, Appl. Catal. 64 (1990) 259.
[7] G.T. Went, L.J. Leu, R.R. Rosin and A.T. Bell, J. Catal. 134 (1992) 492.
[8] U.S. Ozkan, Y. Cai and M.W. Kumthekar, J. Catal. 149 (1994) 390.
[9] C.U.I. Odenbrand, A. Bahamonde, P. Avila and J. Blanco, Appl. Catal. B 5 (1994) 117.
[10] N.-Y. Topsøe, J.A. Dumesic and H. Topsøe, J. Catal. 151 (1995) 241.
[11] R.T. Yang, J.P. Chen, E.S. Kikkinides, L.S. Cheng and J.E. Cichanowicz, Ind. Eng. Chem. Res. 31 (1992) 1440.
[12] R.T. Yang and J.E. Cichanowicz, US Patent 5,415,850 (1995).
[13] J.P. Chen, M.C. Hausladen and R.T. Yang, J. Catal. 151 (1995) 135.
[14] R.T. Yang and W.B. Li, J. Catal. 155 (1995) 414.
[15] L.S. Cheng, R.T. Yang and N. Chen, J. Catal. 164 (1996) 70.
[16] H.L. del Castillo, A. Jil and P. Grange, Catal. Lett. 36 (1996) 237.
[17] R.Q. Long and R.T. Yang, J. Catal., submitted.
[18] L.S. Cheng and R.T. Yang, Ind. Eng. Chem. Res. 34 (1995) 2021.
[19] D. Li, A.A. Scala and Y.H. Ma, Adsorption 2 (1996) 227.
[20] R. Mokaya and W. Jones, J. Catal. 153 (1995) 76.
[21] J. Bovey, F. Kooli and W. Jones, Clay Miner. 31 (1996) 501.
[22] S.W. Bailey, in: *Structures of Clay Minerals and Their X-Ray Identification*, Mineralogical Society Monograph, Vol. 5, eds. G.W. Brindley and G. Brown (Mineralogical Society, London, 1980).
[23] M.C. Kung and H.H. Kung, Catal. Rev. Sci. Eng. 27 (1985) 425.
[24] Y.V. Belokopytov, K.M. Kholyavenko and S.V. Gerei, J. Catal. 60 (1979) 1.
[25] T. Yamaguchi, T. Jin and K. Tanabe, J. Phys. Chem. 90 (1986) 3148.